Separation Science and Technology
Publication details, including instructions for authors and subscription information:
http://www.informaworld.com/smpp/title~content=t713708471

Adsorption Equilibrium and Dynamics of C_4 Olefin/Paraffin on π-Complexing Adsorbent

Jae-Wook Lee[a]; Jong-Ho Park[a]; Sang-Sup Han[a]; Jong-Nam Kim[a]; Soon-Haeng Cho[a]; Yong-Taek Lee[b]
[a] Separation Process Research Center, Korea Institute of Energy Research, Yuseong-gu, Daejeon, Korea
[b] Department of Chemical Engineering, Chungnam National University, Yuseong-gu, Daejeon, Korea

To cite this Article Lee, Jae-Wook , Park, Jong-Ho , Han, Sang-Sup , Kim, Jong-Nam , Cho, Soon-Haeng and Lee, Yong-Taek(2005) 'Adsorption Equilibrium and Dynamics of C_4 Olefin/Paraffin on π-Complexing Adsorbent', Separation Science and Technology, 39: 6, 1365 — 1384

To link to this Article: DOI: 10.1081/SS-120030488

URL: http://dx.doi.org/10.1081/SS-120030488

SEPARATION SCIENCE AND TECHNOLOGY
Vol. 39, No. 6, pp. 1365–1384, 2004

Adsorption Equilibrium and Dynamics of C_4 Olefin/Paraffin on π-Complexing Adsorbent

Jae-Wook Lee,[1] Jong-Ho Park,[1] Sang-Sup Han,[1]
Jong-Nam Kim,[1,*] Soon-Haeng Cho,[1] and Yong-Taek Lee[2]

[1]Separation Process Research Center, Korea Institute of Energy
Research, Yuseong-gu, Daejeon, Korea
[2]Department of Chemical Engineering, Chungnam National University,
Yuseong-gu, Daejeon, Korea

ABSTRACT

Ag^+ ion impregnated clay as a newly developed adsorbent was studied for 1-butene separation from *n*-butane. Equilibrium adsorption isotherms of pure components were measured at the temperature range from 25°C to 100°C and pressure up to 1200 mmHg. Experimental data of *n*-butane and 1-butene were correlated with various isotherm models. The best selectivity was shown at 80°C. Equilibrium capacities for 1-butene and *n*-butane at 80°C and 900 mmHg were 0.92 and 0.31 mmol/g, respectively. The average heats of adsorption for *n*-butane and 1-butene were found

---

*Correspondence: Jong-Nam Kim, Separation Process Research Center, Korea Institute of Energy Research, 71-2 Jang-dong, Yuseong-gu, Daejeon 305-243, Korea; Fax: 82-42-860-3102; E-mail: jnkim@kier.re.kr.

DOI: 10.1081/SS-120030488 0149-6395 (Print); 1520-5754 (Online)

www.dekker.com

to be 6.6 and 13.3 kcal/mol, respectively. Diffusion of 1-butene and *n*-butane on this sorbent was fast, with 100% uptake reached within 15 min. The IAS model with Toth isotherm for pure component gave the best prediction results for both the *n*-butane and 1-butene compared to the other models used in the study. Binary adsorption equilibrium was well predicted by the Ideal Adsorbed Solution (IAS) model. The equilibrium adsorption ratio of 1-butene/*n*-butane in binary system was 14.87 and its selectivity was 6.71 at 80°C and 900 mmHg, when the mole fraction of 1-butene in gas phase was 0.689. Experimental breakthrough curves were well predicted by a mathematical model, and the curves were steep enough to separate 1-butene from *n*-butane. Thus, it can be noted that Ag^+ ion impregnated clay can be applied to the adsorptive separation of C_4 olefin/paraffin.

Key Words: C_4 Olefin/paraffin separation; $AgNO_3$/clay; Equilibrium capacity; Heat of adsorption; Binary adsorption equilibrium; Breakthrough.

INTRODUCTION

Olefin/paraffin separation represents the most important separation in the petrochemical processes. Cryogenic distillation has been used for over 60 years for these separations.[1] They remain the most energy-intensive distillations because of the close relative volatilities

Residual stream of methyl tertiary butyl ether (MTBE) process contains many important chemicals. This stream mainly consists of 1-butene, 2-butene, and *n*-butane. Butene-1 is an important chemical intermediate used in the manufacture of a variety of chemical products, i.e., linear low density polyethylene (LLDPE), high density polyethylene (HDPE), polypropylene (PP), and synthetic lubricants. The C_4 components in this stream cannot be easily separated by conventional distillation because of the close proximity of the boiling points. The superfractination, which is the existing technique to separate C_4 components, is a complex process and its energy consumption is high. Even though the hybrid system that consists of simulated moving bed and distillation tower was applied as an advanced technique, it was also a complex and energy intensive process.[2,3]

Currently, a number of alternative methods have been investigated for the olefin/paraffin separation.[4] The most attractive one is adsorption. Since satisfactory selectivity for olefin/paraffin has not been shown on commercial sorbents, i.e., zeolite 5A and 13X, the new sorbents using π-complexing agents have generated considerable research interest.[5] The use of complex ing agent can be classified into three forms: solution,[6] solid adsorbent, and membrane.[7] The advantage of chemical bond by π-complexation is that the bond formed is stronger than that by van der Waals force alone, so it is possible to achieve high selectivity and weak enough to be broken by simple engineering operation such as raising temperature or decreasing the pressure. These advantages have been highlighted through a molecular orbital study of the selective adsorption on Ag^+- and Cu^+-exchanged resins.[8,9] π-Complexation pertains to the main-group (d-block) transition metals on the periodic table. These metals or their ions can form a σ-bond to carbon and the unique characteristics of the d orbital in these metals or ions can form bonds with olefins by backdonation.[10]

More recently, a number of π-complexation adsorbents have been developed for olefin/paraffin separations.[11–14] These include Ag^+-exchanged resins and $AgNO_3/SiO_2$. Other types as a substrate for π-complexation sorbents are pillared clays. These are a new class of aluminosilicate material, which have attracted increasing interest for both adsorption and catalysis because of their unique structural and chemical properties.[15,16] These π-complexation sorbents provided excellent results for olefin separation from paraffin. But, these researches were limited to C_2 and C_3 hydrocarbon separation, i.e., ethylene/ethane and propylene/propane. Even though Padin et al.[18] researched to separate 1-butene/*n*-butane on $AgNO_3/SiO_2$ of which weight ratio was 1.08, and it had a good selective adsorption ratio of 8.33 for 1-butene/butane at 70°C and 1 atm, the study was limited to adsorption characteristics of C_4 pure components, not binary system and dynamics in packed column. Thus, in this work, we have studied the feasibility of the π-complexation sorbents, $AgNO_3$/clay, for the separation of 1-butene from *n*-butane. Pure component isotherms were measured at various temperature range on Ag^+ impregnated clay as a newly developed adsorbent. To make sure that it has enough selectivity of 1-butene/*n*-butane, binary experiment was carried out at 80°C and 900 mmHg. The dynamics in packed column with $AgNO_3$/clay was studied in order to develop adsorption process for separation of C_4 olefin/paraffin.

EXPERIMENTAL SECTION

Newly developed adsorbent for C_4 olefin/paraffin separation is synthesized by effective dispersion of Ag^+ on granular type clay. $AgNO_3$ is dispersed on a clay surface using the incipient wetness technique. That is, just the same amount of $AgNO_3$ solution as the pore volume of substrate was contacted with the adsorbent during the impregnation stage. The clay substrate used in this study was granular form (particle size of 8–12 mesh). $AgNO_3$/clay at a weight ratio of 0.4 g/g was the sorbent utilized in this work. Table 1 shows the physical properties of clay substrate and $AgNO_3$/clay.

Table 1. Physical properties of clay and $AgNO_3$/clay.

Adsorbent	Average pore diameter (Å)	Surface area (m^2/g)	Pore volume (cm^3/g)
Clay substrate	40.33	391.24	0.42
$AgNO_3$/clay	52.19	132.86	0.20

Since Ag^+ ion impregnated on clay substrate blocks the mouth of micropore, $AgNO_3$/clay has large pore diameter and smaller surface area and pore volume than clay substrate. Equilibrium amounts adsorbed of 1-butene and *n*-butane were measured at the temperature range from 25°C to 100°C and pressure up to 1200 mmHg using the volumetric method. Temperature was controlled ± 0.5°C by water bath. The schematic diagram of the volumetric apparatus is shown in Fig. 1. At binary system, gas chromatography was connected to the apparatus to analyze a composition in reference cell and sample cell. The binary adsorption equilibrium was measured at 80°C and 900 mmHg. Benedict–Weber–Redlich (BWR) equation of state was used to calculate the moles in the gas phase, since it showed the better result for the densities of C_4 hydrocarbons than other equations of state, i.e., Redlich–Kwong (R–K), Soave–Redlich–Kwong (S–R–K) and virial.[19,20] Magnetic suspension balance (MSB) was used to obtain mass transfer coefficient.

The breakthrough test was done in a column of 1 in. in I.D. and 30 cm in length. *n*-Butane was adsorbed first on $AgNO_3$/clay column before the breakthrough test. The mixed gases of 1-butene and *n*-butane were used as a feed, of which composition ratio was 50 : 50. The feed flow rates were 0.32, 0.64,

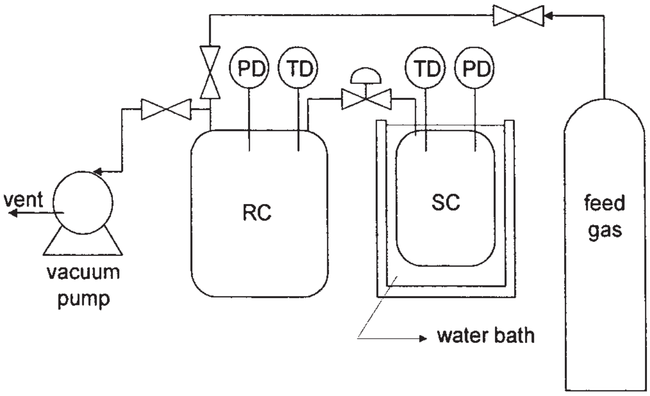

Figure 1. Schematic diagram of the volumetric apparatus.

and 0.96 L/min controlled by mass flow controller (MFC). The adsorption pressure was adjusted by a backpressure regulator. The temperature of adsorber was maintained at 80°C by temperature controller (isothermal condition). The schematic diagram for breakthrough test is shown in Fig. 2.

ISOTHERMS AND MATHEMATICAL MODEL FOR BREAKTHROUGH

Adsorption Equilibrium

The experimental adsorption equilibrium data were correlated with various adsorption isotherm models. Table 2 shows the pure component isotherm models used in this work.[18,21–23] The LRC and Toth models based on the Langmuir isotherm are empirical equations, and the Dubinin–Astakov (D–A) model is based on the potential theory.[17,21,23] The adsorption of olefin molecules on $AgNO_3$/clay is the sum of physical adsorption and

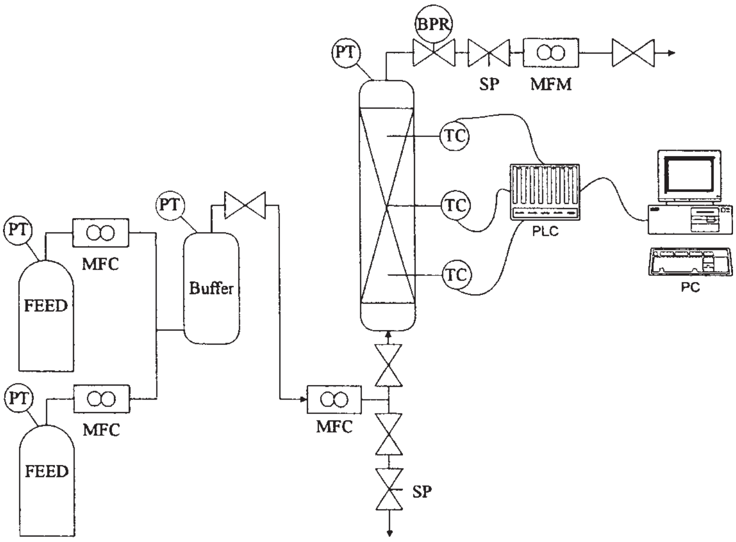

MFC : Mass Flow Controller
MFM : Mass Flow Meter

PT : Pressure Indicator
TC : Thermocouple

BPR : Back Pressure Regulator
SP : Sampling Port

Figure 2. Schematic diagram of breakthrough test apparatus.

Table 2. Isotherm model.[18,21–23]

Langmuir	$q = \dfrac{q_{\mathrm{s}} b_{\mathrm{p}} p}{1 + b_{\mathrm{p}} p}$
LRC	$q = \dfrac{q_{\mathrm{s}} b_{\mathrm{p}} p^n}{1 + b_{\mathrm{p}} p^n}$
Toth	$q = \dfrac{q_{\mathrm{s}} p}{(1/k + p^n)^{1/n}}$
D–A	$q = q_{\mathrm{s}} \exp\left[-\left(C \ln \dfrac{P_{\mathrm{s}}}{P}\right)^m\right]$
LAN + UNILAN	$q = \dfrac{q_{\mathrm{sp}} b_{\mathrm{p}} p}{1 + b_{\mathrm{p}} p} + \dfrac{q_{\mathrm{sc}}}{2s} \ln \dfrac{1 + b_{\mathrm{c}} p \mathrm{e}^{s}}{1 + b_{\mathrm{c}} p \mathrm{e}^{-s}}$

Note: P_s, saturation pressure obtained by the reduced Kirchoff equation at temperatures above the normal boiling point and LAN, Langmuir.

chemisorption. The physical adsorption can be represented by the Langmuir isotherm. Chemisorption is the result of the reversible reaction.[14] In the Langmuir + UNILAN (LAN + UNILAN), the first term accounts for physical adsorption, while the second term represents contribution by chemisorption.[18] The LAN + UNIALN isotherm contains five parameters, and their values may be obtained from the experimental data. However, certain constraints must be imposed on some of the parameters in order for them to have physical meaning. The values of the Langmuir constant are approximately equal between olefin and paraffin with the same carbon number. Therefore, LAN + UNIALN was used to fit the data on π-complexation with imposed values or constraints on q_{sp}, and b_{p}, leaving three parameters (q_{sc}, b_{c}, and s) as the true fitting parameters.[13,18,24]

Many models have been developed for predicting the mixed-gas adsorption equilibria from pure component adsorption isotherms.[25–29] The FastIAS model was used to predict binary adsorption equilibrium.[30–32] The basic equations of IAS (Ideal Adsorbed Solution) is as given below,[28]

$$\frac{\pi A}{RT} = \int_{P=0}^{P=P_i^o} \frac{q_i^o(P)}{P}\,\mathrm{d}P \tag{1}$$

$$\frac{1}{q_t} = \sum_{i=0}^{N} \left[\frac{x_i}{q_i^o(P_i^o)}\right] \tag{2}$$

Also, the Langmuir and the LAN + UNILAN model can be extended to predict binary adsorption equilibrium. If competitive adsorption of n-butane and 1-butene takes place only on clay surface and Ag^+ ion dispersed on clay surface adsorbs only 1-butene, through π-complexation, adsorption equilibria of these two components can be represented by the following equations.

$$q_{n\text{-butane}} = \frac{q_\mathrm{p} b_\mathrm{b} p_i}{1 + \sum b_{\mathrm{p},i} p_i} \tag{3}$$

$$q_{1\text{-butene}} = \frac{q_\mathrm{p} b_\mathrm{b} p_i}{1 + \sum b_{\mathrm{p},i} p_i} + \frac{q_\mathrm{sc}}{2s} \ln \frac{1 + b_\mathrm{c} p \mathrm{e}^{s}}{1 + b_\mathrm{c} p \mathrm{e}^{-s}} \tag{4}$$

In above equations, competitive adsorption of *n*-butane and 1-butene on the surface of clay was represented with the extended Langmuir model. If the physical adsorption constants of *n*-butane and 1-butene are same on the surface of clay, the adsorbed amount of *n*-butane will increase linearly with partial pressure of *n*-butane at constant total pressure.

Mathematical Model for Breakthrough

In the practical application of adsorbent, the situation is generally complex. Thus, in order to develop a mathematical model for dynamics in adsorber, the following assumptions are introduced.[17,33]

1. Ideal gas law applies.
2. The flow pattern is plug flow.
3. The system is in isothermal condition.
4. The mass transfer rate can be represented by a linear driving force (LDF) rate expression.

Based on the above assumption, the mass balance for each component of the mixture and the total mass balance were written as follows.
Component mass balance:

$$\frac{\partial y_i}{\partial t} + u \frac{\partial y_i}{\partial z} + \frac{(1-\varepsilon)}{\varepsilon} \rho_\mathrm{p} \frac{RT}{P} \frac{\partial \overline{q_i}}{\partial t} - y_i \sum_i \frac{(1-\varepsilon)}{\varepsilon} \rho_\mathrm{p} \frac{RT}{P} \frac{\partial \overline{q_i}}{\partial t} = 0 \tag{5}$$

Total mass balance:

$$\frac{\partial C}{\partial t} + \frac{\partial (uC)}{\partial z} + \sum_i \frac{(1-\varepsilon)}{\varepsilon} \rho_\mathrm{p} \frac{\partial \overline{q_i}}{\partial t} = 0 \tag{6}$$

Mass transfer rates (LDF):

$$\frac{\partial \overline{q_i}}{\partial t} = k(q_i^* - \overline{q_i}) \qquad k = a\frac{D_e}{R^2} \tag{7}$$

where the rate coefficient, k, is an overall effective mass transfer coefficient as a lumped parameter and a is a constant. The value of D_e/R^2 can be calculated from the following equation. The value of D_e/R^2 can be calculated from the classical solution of the diffusion equation in a sphere.[33]

$$\frac{m_t}{m_\infty} = 1 - \frac{6}{\pi^2}\sum_{n=1}^{\infty}\frac{1}{n^2}\exp\left(-\frac{n^2\pi^2 D_e t}{R^2}\right) \tag{8}$$

Boundary conditions of this system:

$$y_i(0,\ t) = y_{i,\mathrm{in}}, \quad T(0,\ t) = T_{\mathrm{in}}, \quad u(0,\ t) = u_{\mathrm{in}} \quad \text{for } t > 0$$

Initial conditions:

$$y_i(z,\ 0) = 0, \quad T(z,\ 0) = T_w \quad \text{for } 0 \le z \le L$$

To solve the above system of partial differential equations, the spatial derivatives are divided using a backward difference scheme, and resulting ordinary differential equations are solved with the GEAR method.

RESULTS AND DISCUSSION

Isotherms and Kinetics of Pure Components

Pure component adsorption isotherms of n-butane and 1-butene at each temperature on $AgNO_3$/clay are shown in Figs 3 and 4. Table 3 represents absolute average deviation between experimental data and correlated results. The experimental results of n-butane are well correlated with the Langmuir, LRC, Toth, and D–A isotherm. However, in case of 1-butene, not all the models give reasonable prediction performance. Models, which account for the surface heterogeneity such as the LRC, Toth, and D–A, predict the adsorbed amount of 1-butene quite well. But model derived under the assumption of homogeneous surface, the Langmuir model, gives poor prediction results. Considering the two distinctive adsorption sites of $AgNO_3$/clay, i.e., the physical adsorption and π-complexation sites, the above observation is quite natural. The LAN + UNILAN model, which accounts for the physical

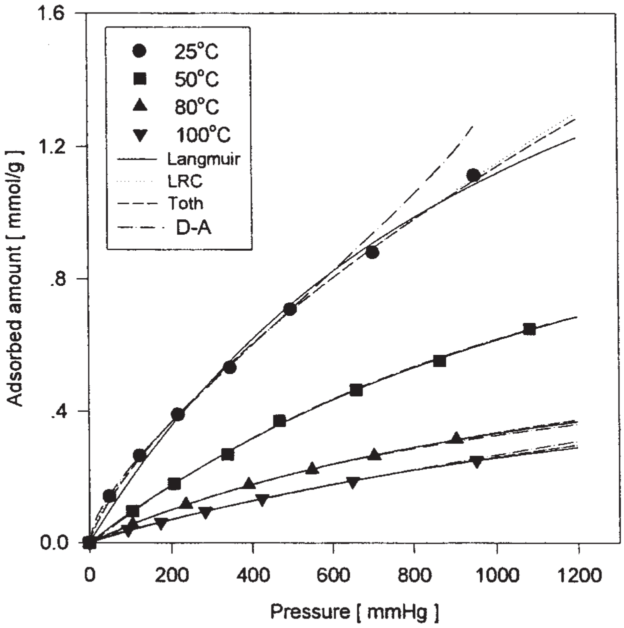

Figure 3. Equilibrium isotherm of *n*-butane (lines are fittings with isotherm model).

adsorption and π-complexation with separate terms, predicts well the adsorbed amount of 1-butene because the model allows to apply different adsorption energy for physical adsorption and π-complexation. Moreover, the UNILAN term is essentially based on the assumption that the adsorbent has uniform adsorption energy distribution. Because of the above characteristics of the model, amount adsorbed of 1-butene was also well predicted by the LAN + UNILAN model. Adsorbed amounts of 1-butene and *n*-butane at 80°C and 900 mmHg were measured at 0.92 and 0.31 mmol/g, respectively.

Figure 5 represents adsorption ratio of $q_{1\text{-butene}}/q_{n\text{-butane}}$ for pure component at each temperature. As shown in figure, adsorption ratio exponentially decreases with pressure. It has the highest value at 80°C, but the differences of adsorption ratio at 80°C and 100°C over 600 mmHg becomes smaller. Thus, binary isotherm experiment was carried out at 80°C and 900 mmHg. Table 4 represents adsorption ratio of $q_{1\text{-butene}}/q_{n\text{-butane}}$ at each temperature and 900 mmHg.

Figure 6 shows the isosteric heat of adsorption of each component calculated from isotherm model using Van't Hoff equation.[20] The average heats of adsorption for *n*-butane and 1-butene are found to be 6.6 and 13.3 kcal/mol,

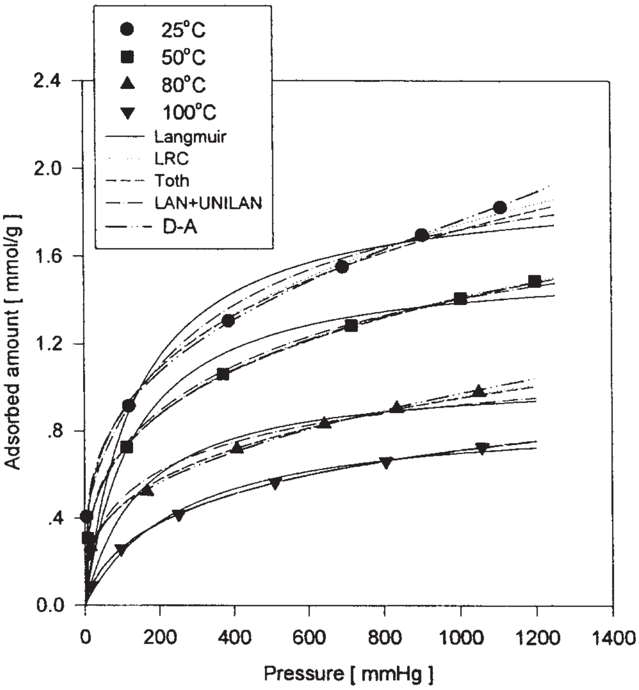

Figure 4. Equilibrium isotherm of 1-butene (lines are fittings with isotherm model).

respectively. As the adsorbed amount increases, the heat of adsorption decreases since the site, which has higher adsorption energy, is occupied first by the adsorbate.

Figure 7 shows the adsorption rates of 1-butene and *n*-butane on $AgNO_3$/clay at 80°C. For all uptake curves, diffusion of 1-butene and *n*-butane was nearly completed within 15 min. The adsorption rate of 1-butene is slightly faster than *n*-butane. The values of D_e/R^2 of *n*-butane and 1-butene calculated from Eq. (8) are 3.42×10^{-2} and 1.75×10^{-2}/sec, respectively.

Binary Adsorption Equilibrium

Table 5 shows the results of binary isotherm experiment at 80°C and 900 mmHg. The adsorption ratio of 1-butene/*n*-butane is 14.87 and its selectivity is 6.71 when mole fraction of 1-butene in gas phase is 0.689. Thus, it shows enough selectivity to separate 1-butene from *n*-butane on $AgNO_3$/clay.

Table 3. Absolute average deviation (AAD) between experimental data and correlated result (%).

	1-Butene					*n*-Butane			
Temperature (°C)	Langmuir	LRC	Toth	LAN + UNIALN	D–A	Langmuir	LRC	Toth	D–A
25	17.65	2.60	3.55	4.34	0.51	8.34	1.66	2.95	3.52
50	15.23	0.33	0.84	0.86	0.42	1.40	1.30	1.38	1.64
80	14.75	2.11	2.82	1.87	1.05	0.94	1.19	1.26	0.68
100	9.54	0.51	0.60	1.50	0.58	2.58	1.66	2.10	1.80

Note: AAD (%) = $\sum|\text{exp.} - \text{cal'd}|/\text{exp.} \times 100/\text{No. of data}$.

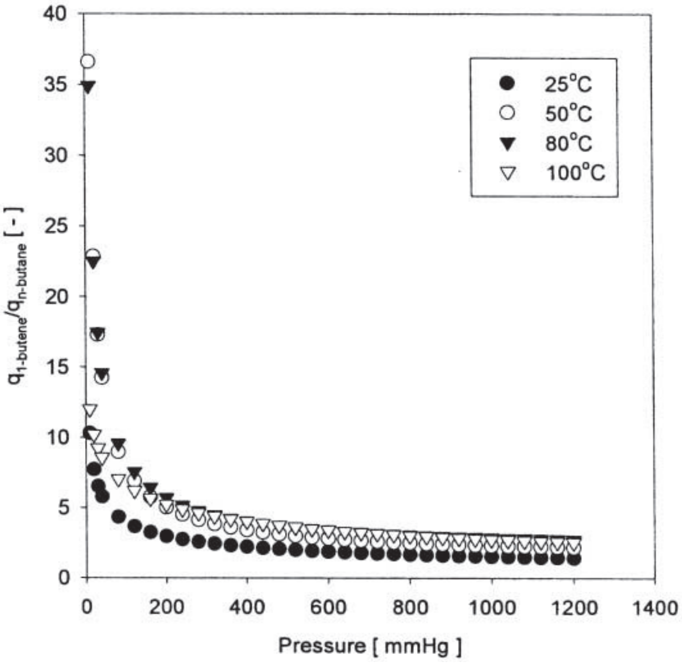

Figure 5. Adsorption ratio of $q_{1\text{-butene}}/q_{n\text{-butane}}$ of pure component.

Figure 8 represents the comparison of experimental results and predicted ones for adsorbed amount and composition at 80°C and 900 mmHg. As the composition of 1-butene in gas phase is increased, the curvatures of binary system are drastically changed. It is noted that the adsorbed amount of *n*-butane is greatly diminished as mole fraction of 1-butene in gas phase increases from 0 to 0.1 and then decreases slowly

Table 4. Adsorption ratio of $q_{1\text{-butene}}/q_{n\text{-butane}}$ at each temperature and 900 mmHg.

Temperature (°C)	$q_{1\text{-butene}}/q_{n\text{-butane}}$ (—)
25	1.58
50	2.37
80	2.94
100	2.86

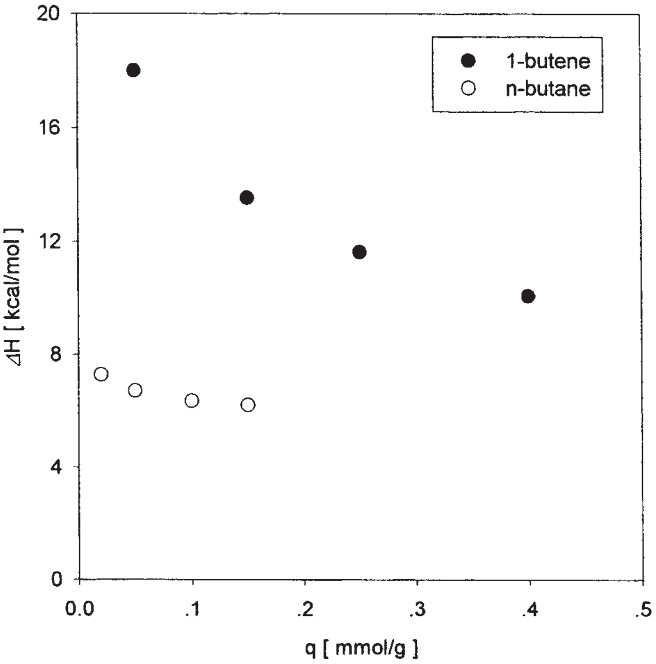

Figure 6. Isosteric heat of adsorption of 1-butene and *n*-butane.

above 0.1. The IAS model with the Toth isotherm for pure component gives the best prediction results for both the *n*-butane and 1-butene compared to the other two models. The same IAS model with the Langmuir isotherm for pure component did not predict the binary equilibrium well especially the amount adsorbed of *n*-butane. In the case of the extended LAN + UNILAN model, adsorbed amount of *n*-butane has a great deviation between experimental results and predicted ones. It is noted that the extended LAN + UNILAN model can explain the adsorbed amount of 1-butene in binary system, however, the extended Langmuir has a limitation to represent the adsorbed amount of *n*-butane.

Adsorption Dynamics in Adsorber

IAS-Langmuir model is used to represent the multi-component adsorption equilibrium, since it predicts binary system better than extended Langmuir + UNILAN model and it is easier to computate dynamics than IAS-Toth. The

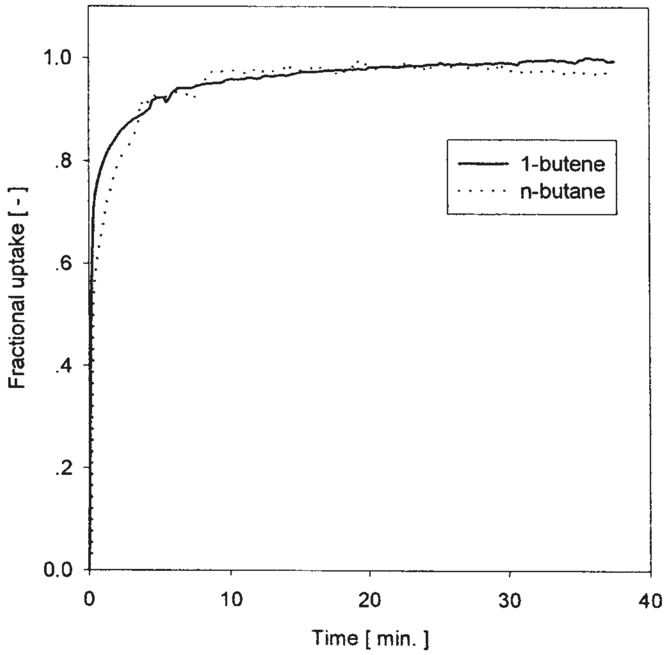

Figure 7. Uptake rates (at $P = 50\,\text{mmHg}$) of 1-butene and n-butane on $AgNO_3$/clay at 80°C.

isotherm parameters are listed in Table 6, and other parameters used in the mathematical model are listed in Table 7. The comparison of experimental data of breakthrough and theoretical results at various flow rates is shown in Fig. 9. The change of flow rate has little effect on the forms of breakthrough curves, and the breakthrough curves are steep enough to separate 1-butene from *n*-butane. In order to produce high purity 1-butene, the adsorbed

Table 5. Binary experimental result at 80°C and 900 mmHg.

$y_{1\text{-butene}}$ (—)	$x_{n\text{-butane}}$ (—)	$x_{1\text{-butene}}$ (—)	$q_{n\text{-butane}}$ (mmol/g)	$q_{1\text{-butene}}$ (mmol/g)	$q_{1\text{-butene}}/q_{n\text{-butane}}$ (—)
0.000	1.000	0.000	0.284	0.000	0.000
0.002	0.657	0.343	0.172	0.090	0.523
0.065	0.302	0.698	0.114	0.262	2.307
0.270	0.118	0.882	0.073	0.545	7.471
0.689	0.063	0.937	0.054	0.805	14.870

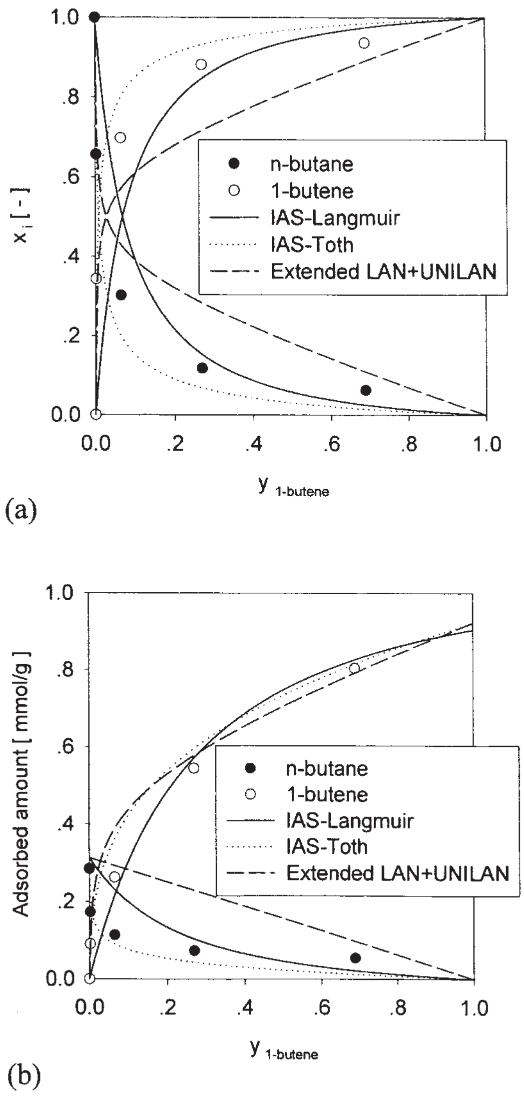

Figure 8. Binary adsorption equilibrium: (a) composition and (b) adsorbed amount.

Table 6. Langmuir parameters of each component.

	Langmuir parameter	
	q_p (mmol/g)	b_p (1/mmHg)
n-Butane	0.7923	7.2419×10^{-4}
1-Butene	1.0576	6.5645×10^{-3}

bed with feed mixture of 1-butene and *n*-butene is rinsed with some part of product, and then desorbed to the product. It is noted that the mathematical model using the IAS-Langmuir provides reasonable fits to the experimental breakthrough curves, although deviation between experimental results and predicted ones is slightly increasing as the feed flow rates decrease. From the results, it can be concluded that the mathematical model proposed in this study provides a good representation of the experimentally observed behavior of breakthrough curves.

CONCLUSION

Newly developed adsorbent for C_4 olefin/paraffin separation was synthesized by impregnating $AgNO_3$ on clay substrate. Equilibrium capacities for 1-butene and *n*-butane at 80°C and 900 mmHg were measured at 0.92 and 0.31 mmol/g, respectively. The experimental data of *n*-butane were correlated well with the Langmuir, LRC, Toth, and D–A. Also, LAN + UNILAN model was adapted to represent both chemisorption and physical adsorption of 1-butene. The average heats of adsorption for *n*-butane and 1-butene were found to be 6.6 and 13.3 kcal/mol, respectively. Diffusion of 1-butene and *n*-butane on this sorbent was fast, with 100% uptake reached within 15 min. Binary isotherm experiment was carried out at 80°C and 900 mmHg. The adsorption ratio of 1-butene/*n*-butane was found to be 14.87 and its selectivity 6.71 when mole fraction of 1-butene

Table 7. Characteristics of adsorption bed and adsorbent.

Bed I.D. (cm)	2.593	Particle density (g/cm^3)	1.7727
Bed O.D. (cm)	3.095	Void fraction (—)	0.4
Bed height (cm)	30.0	Porosity (—)	0.35

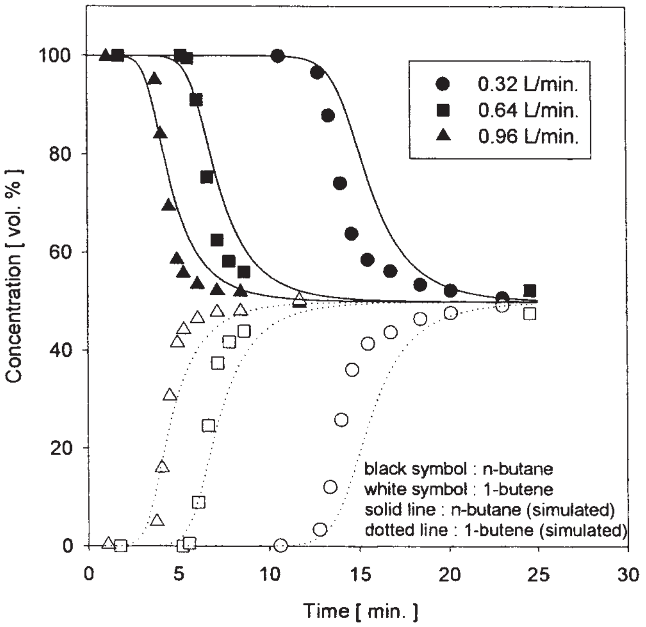

Figure 9. Comparison of experimental data and simulated result of breakthrough curve on $AgNO_3$/clay with various flow rates (feed composition: 50% *n*-butane + 50% 1-butene; $T = 80°C$; $P = 900\,mmHg$).

in gas phase was 0.689 in the binary system. The IAS model with Toth isotherm for pure component gives the best prediction results for both the *n*-butane and 1-butene compared to the other models used in the study. Also, to confirm that 1-butene can be separated from *n*-butane on $AgNO_3$/clay, breakthrough test was carried out. The breakthrough curves were steep enough to separate 1-butene from *n*-butane.

SYMBOLS

q	adsorbed amount, mmol/g
q_s	saturation amount adsorbed, mmol/g
b_p	isotherm parameter, 1/mmHg
m_t	adsorbed amount at time *t*, mg
m_∞	adsorbed amount at equilibrium, mg
n	LRC and Toth isotherm parameter

k	Toth parameter, overall effective mass transfer coefficient
s	heterogeneity parameter of energy distribution
t	time, sec
u	interstitial velocity, cm/sec
z	distance along the length of the column, cm
$\overline{q_i}$	amount adsorbed of ith component, mmol/g
q_i^*	equilibrium amount adsobed, mmol/g
C	gas phase concentration, mmol/cm^3, D–A model parameter
T	temperature, K
P	pressure, mmHg
P_s	saturation pressure at temperatures above the normal boiling point
y_i	mole fraction of ith component in the gas phase
R	gas constant, intraparticle radius
ε	mean of uniform energy distribution, void of packing
ρ_p	particle density, g/cm^3

REFERENCES

1. Keller, G.E.; Marcinkowsky, A.E.; Verma, S.K.; Williamson, K.D. Olefin recovery and purification via silver complexation. In *Separation and Purification Technology*; Li, N.N., Calo, J.M., Eds.; Marcel Dekker: New York, 1992; 59–83.
2. DeRosset, A.J.; Priegnitz, J.W.; Korous, D.J.; Broughton, D.B. Continuous adsorptive separation of 1-butene from C_4-hydrocarbon mixtures, ACS Anaheim Meeting, March 12–17, 1978; 1081; 766–774.
3. Priegnitz, J.W.; Elgin III. The Selective Separation of Butene-1 from C_4 Hydrocarbon Mixture Employing Zeolites X and Y. US Patent 3723561, March 27, 1973.
4. Eldridge, R.B. Olefin/paraffin separation technology: a review. Ind. Eng. Chem. Res. **1993**, *32*, 2208–2212.
5. Chen, J.P.; Yang, R.T. A molecular orbital study of the selective adsorption of simple hydrocarbon molecules on Ag^+- and Cu^+-exchanged resins and cuprous halides. Langmuir **1995**, *11* (9), 3450–3456.
6. Ho, W.S.W.; Doyle, G.D.; Savage, D.W.; Pruett, R.L. Olefin separation via complexation with cuprous diketonate. Ind. Eng. Chem. Res. **1988**, *27* (2), 334–337.
7. Yang, J.S.; Hsiue, G.H. Selective olefin permeation through Ag(I) contained rubber-graft-poly(acrylic acid) membranes. J. Mem. Sci. **1997**, *126* (1), 139–149.

Marcel Dekker, Inc.
270 Madison Avenue, New York, New York 10016

8. Huang, Y.Y. Ethylene complexes in copper(I) and silver(I) Y zeolite. J. Cat. **1980**, *61*, 461–476.
9. Yates, D.J.C. On the location of adsorbed ethylene in a zeolite. J. Phy. Chem. **1966**, *70*, 3693.
10. Cotton, F.A.; Wilikinson, G.; Murillo, C.A.; Bochmann, M. The elements of the second and third transition series. In *Advanced Inorganic Chemistry*, 6th Ed.; Wiley-Interscience: New York, 1999; 1084–1097.
11. Han, S.S.; Kim, J.N.; Cho, S.H. Adsorbents for Light Alkane/Alkene Separation, The 8th APCChE Congress, Seoul, Korea, Aug. 16–19, 1999.
12. Rege, S.U.; Padin, J.; Yang, R.T. Olefin/paraffin separation by adsorption: π-complexation vs. kinetic separation. AIChE **1998**, *44* (4), 799–809.
13. Wu, Z.; Han, S.S.; Cho, S.H.; Kim, J.N.; Chue, K.T.; Yang, R.T. Modification of resin-type adsorbents for ethane/ethylene separation. Ind. Eng. Chem. Res. **1997**, *36* (7), 2749–2756.
14. Yang, R.T.; Kikkinides, E.S. New sorbents for olefin/paraffin separations by adsorption via π-complexation. AIChE **1995**, *41* (3), 509–517.
15. Yang, R.T.; Baksh, M.S.A. Pillared clays as a new class of sorbents for gas separation. AIChE **1991**, *37* (5), 679–686.
16. Chen, L.S.; Yang, R.T. Monolayer cuporous chloride dispersed on pillared clays olefin–paraffin separation by π-complexation. Adsorption **1995**, *1*, 61.
17. Yang, R.T. Adsorbents and adsorption isotherms. In *Gas Separation by Adsorption Processes*; Butterworths: New York, 1987; 26–48, 141–200.
18. Padin, J.; Yang, R.T.; Munson, C.L. New sorbents for olefin/paraffin separations and olefin purification for C_4 hydrocarbons. Ind. Eng. Chem. Res. **1999**, *38* (10), 3614–3621.
19. Perry, R.H.; Green, D. Physical and chemical data. In *Perry's Chemical Engineers' Handbook*, 6th Ed; McGraw-Hill; 1984.
20. Reid, R.C.; Prausnitz, J.M.; Poling, B.E. Pressure–volume–temperature relations of pure gases and liquids. In *The Properties of Gases & Liquids*, 4th Ed.; McGraw-Hill: New York, 1988; 29–69.
21. Do, D.D. Fundamentals of pure component adsorption equilibria. In *Adsorption Analysis: Equilibria and Kinetics*, Series on Chemical Engineering, Imperial College Press: London, 1998; Vol. 2, 13–70.
22. Rege, S.U. Studies in Gas Separation by Pressure Swing Adsorption and Ultrasonic Regeneration of Adsorbents; Univ. Michigan; 2001, Ph.D. Thesis.
23. Valenzuela, D.P.; Myers, A.L. Adsorption of pure gases. In *Adsorption Equilibrium Data Handbook*; Prentice-Hall: New Jersey, 1989; 6–16.

24. Park, J.H.; Lee, H.K.; Han, S.S.; Kim, J.N.; Cho, S.H. Adsorption equilibrium of ethane/ethylene on $AgNO_3$/clay adsorbent. HWAHAK KONGHAK **2002**, *40* (4), 467.
25. Grant, R.J.; Manes, M. Adsorption of binary hydrocarbon gas mixtures on activated carbon. Ind. Eng. Chem. Fundam. **1966**, *5* (4), 490.
26. Myers, A.L.; Prausnitz, J.M. Thermodynamics of mixed-gas adsorption. AIChE **1965**, *11* (1), 121.
27. Suwanayuen, S.; Danner, R.P. A gas adsorption isotherm equation based on vacancy solution theory. AIChE **1980**, *26* (1), 68.
28. LeVan, M.D.; Vermeulen, T. Binary Langmuir and freundlich isotherms for ideal adsorbed solutions. J. Phys. Chem. **1981**, *85* (22), 3247.
29. Talu, O.; Zwiebel, I. Multicomponent adsorption equilibria of nonideal mixture. AIChE **1986**, *32* (8), 1263.
30. Myers, A.L.; Valenzuela, D. Computer algorithm and graphical method for calculating adsorption equilibria of gas mixture. J. Chem. Eng. Jpn. **1986**, *19* (5), 392.
31. O'Brien, J.A.; Myers, A.L. Rapid calculation of multicomponent adsorption equilibriua from pure isotherm data. Ind. Eng. Chem. Process Des. Dev. **1985**, *24* (4), 1188.
32. O'Brien, J.A.; Myers, A.L. A comprehensive technique for equilibrium calculation in adsorbed mixtures: the generalized fastIAS method. Ind. Eng. Chem. Res. **1988**, *27*, 2085.
33. Ruthven, D.M. Dynamics of adsorption columns. In *Principles of Adsorption and Adsorption Processes*; Wiley-Interscience: New York, 1984; 220–272.

Received April 2003
Revised November 2003

Downloaded At: 10:09 25 January 2011

Request Permission or Order Reprints Instantly!

Interested in copying and sharing this article? In most cases, U.S. Copyright Law requires that you get permission from the article's rightsholder before using copyrighted content.

All information and materials found in this article, including but not limited to text, trademarks, patents, logos, graphics and images (the "Materials"), are the copyrighted works and other forms of intellectual property of Marcel Dekker, Inc., or its licensors. All rights not expressly granted are reserved.

Get permission to lawfully reproduce and distribute the Materials or order reprints quickly and painlessly. Simply click on the "Request Permission/ Order Reprints" link below and follow the instructions. Visit the U.S. Copyright Office for information on Fair Use limitations of U.S. copyright law. Please refer to The Association of American Publishers' (AAP) website for guidelines on Fair Use in the Classroom.

The Materials are for your personal use only and cannot be reformatted, reposted, resold or distributed by electronic means or otherwise without permission from Marcel Dekker, Inc. Marcel Dekker, Inc. grants you the limited right to display the Materials only on your personal computer or personal wireless device, and to copy and download single copies of such Materials provided that any copyright, trademark or other notice appearing on such Materials is also retained by, displayed, copied or downloaded as part of the Materials and is not removed or obscured, and provided you do not edit, modify, alter or enhance the Materials. Please refer to our Website User Agreement for more details.

Request Permission/Order Reprints

Reprints of this article can also be ordered at

http://www.dekker.com/servlet/product/DOI/101081SS120030488